energy&fuels

pubs.acs.org/EF

Article

Addressing Thermal Behavior and Molecular Architecture of Asphaltenes by a Thermal-Optical Carbon Analyzer Coupled to High-Resolution Mass Spectrometry

Christopher P. Rüger,* Anika Neumann, Paul Kösling, Silvia Juliana Vesga Martínez, Martha Liliana Chacón-Patiño, Ryan P. Rodgers, and Ralf Zimmermann

Cite This: *Energy Fuels* 2022, 36, 10177−10190

Read Online

ACCESS | Metrics & More | Article Recommendations | Supporting Information

ABSTRACT: In the past decade, extensive molecular-level research on asphaltenes, primarily based on mass spectrometric approaches, acknowledged the coexistence of two primary architecture motifs, "island" single-core- and "archipelago" (multi-core)-type structures. Nonetheless, analytical methods for a classification are still limited. In this study, the thermal desorption and pyrolysis behavior of a diverse set of asphaltenes covering island- and archipelago-enriched samples and their extrographic fractions has been investigated by a thermal-optical carbon analyzer (TOCA) hyphenated to high-resolution mass spectrometric evolved gas analysis. The capability of the TOCA for a temperature-resolved quantification of the released carbon is used together with the option of applying an inert or oxidative atmosphere. We found that the relative proportion of organic carbon emitted under an inert atmosphere and below 580 °C ($OC_{des/pyr}$) and the organic carbon released at elevated temperatures (>580 °C) and oxidative atmosphere ($OC_{pyrogen}$) can be used as a classification approach for the prevalent architecture motif. This finding is likely caused by differences in the coking and charring behavior dependent on molecular structure. Hypothetically, single-core constituents will form more resistive shot-like coke due to their larger aromatic cores, whereas multi-core constituents seem to produce easier combustible sponge-like coke. Simultaneously, resonance-enhanced multiphoton ionization (REMPI), a soft ionization scheme particularly selective and sensitive for aromatic constituents, together with Orbitrap Fourier-transform mass spectrometry, allowed for time/temperature-resolved in-depth insights into the evolved chemistry. The alkylation pattern/length of the mass spectra received in $OC_{des/pyr}$ (480/580 °C) fractions has been identified as a classification measure with lower and more narrow patterns for the asphaltenes dominated by single-core species. However, grouping based on the quantified TOCA results has been significantly more striking. Conclusively, TOCA of asphaltenes and their extrographic fractions can be used for structural classification as well as insights into coprecipitated maltenes, presumably also successfully applicable in future studies on residues from renewable oil sources.

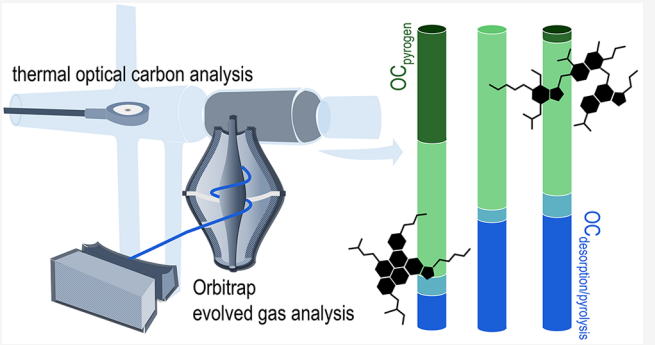

INTRODUCTION

Unraveling the structural moieties of complex organic samples on a molecular level remains a grand challenge for analytical chemistry. In this respect, materials of fossil origin have been found to be one of the world's most complex mixtures and, thus, an ideal candidate for analytical method development in the past decades. In particular, high-resolution mass spectrometry (HRMS) has proven to be a powerful method facilitating in-depth molecular level insights in complex mixtures.[1−3] Although previous research focused on fossil-derived materials, due to the changing landscape of fuels, novel biofuel developments,[4,5] and stronger focus on circular economies/recycling,[6] this research field is in a steady transformation. However, it remains focused on carbon-based fuels, as they will remain the dominate energy source for transportation (i.e., shipping/aviation) in the foreseeable future.[7] To combat climate change and, thus, lower the carbon dioxide emissions, future fuels will be increasingly based on renewable sources.

However, despite the inevitable shift toward green energy production, substantial global research in material science utilization of classical fossil sources can be seen. In fossil petroleum refining, flow assurance is one of the common challenges due to deposit formation, flocculation, or catalyst poisoning.[8−10] As a key contribution to a variety of problems,

Received: June 26, 2022
Revised: August 12, 2022
Published: August 21, 2022

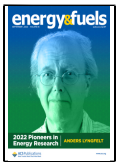

https://doi.org/10.1021/acs.energyfuels.2c02122
Energy Fuels 2022, 36, 10177−10190

the fraction of petroleum termed "asphaltenes" has been identified.[11−13] Asphaltenes are defined as *n*-pentane/*n*-heptane insoluble fraction of crude oil likely containing high molecular weight, heteroatom-rich and highly aromatic compounds, which are prone to aggregation, and complex occlusion inter- and intramolecular interactions with other oil fractions.[14−16] Despite their problematic nature with regard to petroleum processing, asphaltenes are currently gaining importance in material sciences for the generation of carbon fibers.[17] They also have potential as supercapacitors,[18,19] as novel materials when chemically modified, e.g., by cross-linking,[20] or for liquid purification.[21] Thus, utilizing fossil resources in material science will coincide with lowering the carbon dioxide emissions, while still being able to supply the global economy with affordable products. For all these novel applications, a molecular-level knowledge of the chemical composition of heavy petroleum fractions is a prerequisite for directed development. Nonetheless, the molecular composition and architecture of asphaltenes remains heavily discussed in the community and is far from entirely unraveled.[22] Two architecture models have been proposed as dominant structural motifs: large aromatic moieties with alkyl side chains referred to as "island" single-core structures and bridged aromatic "archipelago" multi-core structures.

From the physicochemical perspective, the predominance of multi- or single-core species will highly influence the reaction properties of asphaltenes. In general, thermal cracking at elevated temperatures above 400 °C has shown high contributions of aromatic and heteroaromatic species with one- to four-rings along with alkanes, alkenes, and naphthenic species.[23−26] Recently, the role of "island" and "archipelago" motifs was investigated with respect to the hydroconversion of distillable products, revealing a strong structure−reactivity relationship.[27] The coking yield, as a central parameter for economic valorization, was found to have a complex dependence on the aromatic structures and molecular functionalities. Consequently, knowledge of the structural architecture of asphaltenes is central for predicting not only the resulting chemistry in classical refining conversion workflows but also in material science utilization. Hence, there is a strong need for an analytical descriptor that provides information to the predominant molecular motif in such ultracomplex mixtures.

High-resolution Fourier transform ion cyclotron resonance mass spectrometry (FT-ICR MS) has been established as a widely used technique for the characterization of asphaltenes on the molecular level.[22,28] Here, the high mass accuracy (subppm) and resolving power is routinely utilized for unambiguous elemental composition attribution. Direct mass spectrometric analysis provides limited structural information, such as by elemental composition and derived measures, e.g., double bond equivalents (DBE), aromaticity index (AI), or carbon oxidation state (OS_C). Hence, custom fragmentation and separation approaches combined with state-of-the-art mass spectrometry have been extensively used over the past decade for a deeper insight into asphaltene structural diversity.[22,29,30] Recently, Chacón-Patiño et al. used FT-ICR MS combined with infrared multiphoton dissociation (IRMPD) to thermally fragment a preselected narrow mass window (quadrupole m/z windowing).[22] The applied infrared laser causes heating of the molecules in the gas phase, and fragmentation is performed in an ultrahigh vacuum, in which secondary reactions are unlikely. This technique was successfully employed in a number of studies to solve the structural debate on complex asphaltene samples.[31−33] Thermal analysis mass spectrometry, which heats the sample prior to ionization and subsequent mass spectrometric analysis, has also revealed great potential for describing petroleum and its SARA fractions.[15,34−37] Here, asphaltenes have been studied in combination with different kinds of mass analyzers and ionization schemes, which can be recognized as a complementary attempt to the IRMPD approach.[15,36] Thermogravimetry coupled to FT-ICR MS uniquely revealed the differences in coking behavior and presence of occluded material comparing different extrographic fractions of Wyoming (enriched in island motif) and Athabasca (enriched in archipelago motif) asphaltenes.[15] Significant yields of cracked side chains and dealkylated aromatics have been consistent with single-core structures for the Wyoming deposit and are distinctly different to the evolved molecular pattern of the multi-core-enriched Athabasca bitumen asphaltenes. Thermogravimetry was able to quantify the temperature-resolved mass loss and residual masses; however, the direct quantification of the individual species in each is not currently possible.

In environmental sciences, thermal-optical carbon analysis (TOCA) is a common classification approach for particulate matter (PM).[38] TOCA allows for quantitative determination of carbon fractions (total carbon, TC; organic carbon, OC; and elemental carbon, EC) of a sample collected/deposited on a quartz fiber filter.[39] The sample is heated in a programmable oven with an adjustable inert or oxidative atmosphere. Released material is transferred to an oxidative oven converting the carbonaceous species to carbon dioxide, which is subsequently quantified, e.g., by a near-infrared spectroscopic detector. In a simplified perspective, carbon released under inert conditions is referred to as organic carbon, whereas carbon evolved from treatment under an oxidative atmosphere is considered as elemental carbon.[39] Several thermal protocols have been proposed, such as the NIOSH5040 or IMPROVE_A methodology.[40,41] An advantage of TOCA compared to thermogravimetric analysis is the possibility to directly quantify the released carbon fractions. Furthermore, also coke formed during the pyrolysis steps is accessible when the atmosphere is changed to oxidative condition at elevated temperatures. A fraction of the evolved gas mixture can be transferred to mass spectrometric analysis, allowing for further insights into the chemistry of the evolved species.[42,43] This concept has been extensively used for PM and also for petroleum-derived fuels, such as heavy fuel oils, and other complex carbonaceous matrixes.[44−46] In contrast to thermogravimetric analysis, no information on the mass loss can be received.

This study evaluates the hyphenation of a thermal-optical carbon analyzer with evolved gas analysis by high-resolution mass spectrometry for the characterization of asphaltenes. As the molecular architecture strongly influences the coking behavior of a given heavy residue or asphaltene fraction, we hypothesize that the organic and elemental carbon values serve as an overview measure, thus giving an indirect descriptor for the predominant asphaltene structural motif. Analysis of the evolved gas mixture is carried out by a recently introduced Orbitrap high-resolution mass analyzer equipped with sensitive and soft vacuum photoionization.[47] Particularly, photoionization techniques have shown to be less prone to matrix effects and ion suppression, with vacuum ionization schemes at the forefront revealing a low bias. Here, resonance-enhanced multiphoton ionization (REMPI) selectively addresses aro-

https://doi.org/10.1021/acs.energyfuels.2c02122
Energy Fuels 2022, 36, 10177−10190

Table 1. Overview of the Crude Oil and Asphaltene Sample Material Investigated in This Study[a]

name	abbreviation	description	classification
PetroPhase 2017 parent crude oil	PP crude oil	parent crude oil used for the interlaboratory study of the PetroPhase 2017 conference[16,48]	
PetroPhase 2017 asphaltene	PP asph	asphaltene used for the interlaboratory study of the PetroPhase 2017 conference[16,48]	slightly archipelago-enriched[32]
heavy oil C5 asphaltene	HO8C5	*n*-pentane asphaltene of a heavy oil by a modified ASTM D6560 method[34,49,50]	unknown
heavy oil C6 asphaltene	HO8C6	*n*-hexane asphaltene of a heavy oil by a modified ASTM D6560 method[34,49,50]	unknown
heavy oil C7 asphaltene	HO8C7	*n*-heptane asphaltene of a heavy oil by a modified ASTM D6560 method[34,49,50]	unknown
Athabasca asphaltene	AA	*n*-heptane asphaltene of Athabasca bitumen by a modified ASTM D6560 method[16,51]	archipelago-enriched[27,33]
Athabasca asphaltene Hep/Tol fraction	AA-Hep/Tol	extrographic fraction of Athabasca asphaltene with *n*-heptane/toluene (1:1, v/v)	archipelago-enriched
Athabasca asphaltene Tol/THF/MeOH fraction	AA-Tol/THF/MeOH	extrographic fraction of Athabasca asphaltene with toluene/tetrahydrofuran/methanol (10:10:1, v/v)	archipelago-enriched
Athabasca asphaltene acetone fraction	AA-Ace	extrographic fraction of Athabasca asphaltene with acetone	archipelago-enriched
Wyoming deposit asphaltene	W	*n*-heptane asphaltene of Wyoming deposit by a modified ASTM D6560 method[16,51]	island-enriched[27,33]
Wyoming deposit asphaltene Hep/Tol fraction	W-Hep/Tol	extrographic fraction of Wyoming deposit asphaltene with *n*-heptane/toluene (1:1, v/v)	island-enriched
Wyoming deposit asphaltene Tol/THF/MeOH fraction	W-Tol/THF/MeOH	extrographic fraction of Wyoming deposit asphaltene with toluene/tetrahydrofuran/methanol (10:10:1, v/v)	island-enriched
Wyoming deposit asphaltene Acetone fraction	W-Ace	extrographic fraction of Wyoming deposit asphaltene with acetone	island-enriched

[a]Classification refers to the asphaltene architecture structural motif with referenced publications. It has to be noted that the Wyoming asphaltene results from an already fractionated Wyoming deposit material.

matic constituents and, thus, was assumed to be ideal for studying the evolved asphaltene aromatic molecules. Well-studied and unknown asphaltene samples, were investigated for broad coverage of asphaltene architecture. In particular, the correlation of the general TOCA results with the temperature-resolved high-resolution mass spectra is presumed to give new insights into the emitted molecular pattern and establish TOCA-MS as a complementary, valuable chemical descriptor for asphaltenes.

EXPERIMENTAL SECTION

Material. In this study, a sample set of 13 fossil petroleum materials have been investigated, composed of one reference crude oil (PetroPhase 2017 parent crude oil) and 12 asphaltenes. The parent crude oil is a Middle Eastern crude oil with an API gravity of 12°.[16] Further information on the different asphaltene samples can be found in Table 1. The sample-set covers materials with enriched in a particular structural motifs, such as the Athabasca asphaltenes, highly enriched in archipelago-type compounds, and Wyoming asphaltenes, highly enriched in island-type structural motifs, the PetroPhase 2017 asphaltene slightly enriched by archipelago-type structures,[32] as well as the heavy oil asphaltene (HO8CX) for which no precise classification is known.

Methods. The analytical platform consists of two parts, a thermal-optical carbon analyzer and a photoionization high-resolution mass spectrometer that provides characterization of the evolved aromatic species through soft and selective ionization. A schematic representation of the hyphenation between thermal-optical carbon analyzer and the high-resolution Orbitrap mass spectrometer is shown in Figure 1. In summary, the analytical platform consists of two parts, a thermal-optical carbon analyzer and a photoionization high-resolution mass spectrometer that provides characterization of the evolved aromatic species through soft, selective ionization. Similar hyphenations have been presented based on time-of-flight mass spectrometry from our group previously.[42,43]

Thermal-Optical Carbon Analyzer. For thermal-optical carbon analysis, the crude oil and asphaltene samples were dissolved in

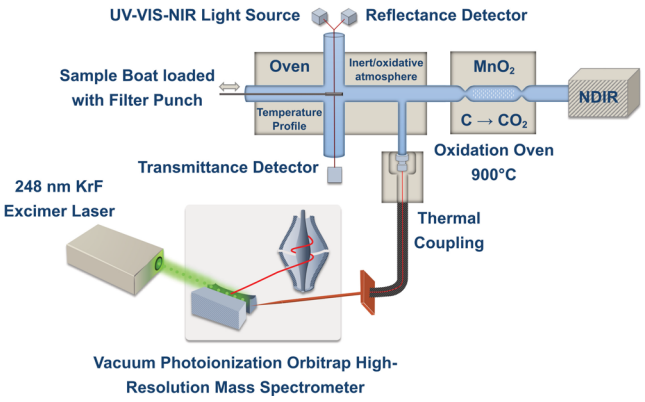

Figure 1. Scheme of the coupling between thermal-optical carbon analyzer and high-resolution mass spectrometer equipped with laser-based vacuum photoionization. Carbon content is determined by a NDIR (nondispersive infrared sensor) that measures CO_2.

dichloromethane (Sigma-Aldrich, LiChrosolv, ≥ 99.9%) to a concentration of 20 mg/mL. Pure DCM was used as a blank. All samples were analyzed using a DRI Model 2015 Series 1 multiwavelength thermal-optical carbon analyzer (TOCA, Aerosol d.o.o.). The instrument was conditioned and calibrated as described by the manufacturer (system pressure, 0.345−0.483 bar; total flow, 180−190 mL/min). A circular punch (8 mm diameter, 0.5 cm^2) of a preconditioned (baked for 6 h at 550 °C) quartz fiber filter (QFF, Whatman QM-A Quartz Microfiber Filters, 47 mm diameter, 0.42 mm thickness) was used to place the blank and asphaltene sample solutions avoiding nonuniform deposits. A sample volume of 5 μL was spotted at the center of the filter using a 10 μL stainless steel manual syringe. After sample application, it was dried (10 s) before insertion of the sample into the TOCA quartz tube. The oven was heated stepwise according to a defined preset temperature program. The thermal analysis protocol used was IMPROVE_A, which defines 140, 280, 480, and 580 °C as temperature plateaus for the fractions OC1−

https://doi.org/10.1021/acs.energyfuels.2c02122
Energy Fuels 2022, 36, 10177−10190

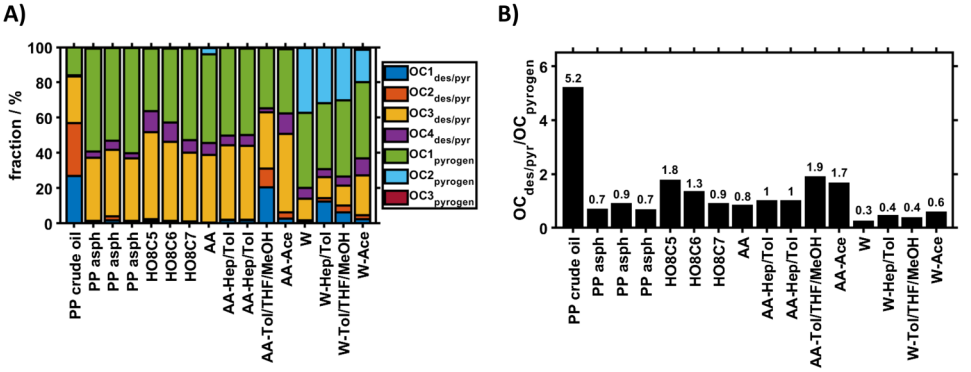

Figure 2. Results of the thermal-optical carbon analysis of the petroleum and asphaltene fractions. (A) Quantified carbon response according to the desorption steps ($OC1_{des/pyr}$ and $OC2_{des/pyr}$), pyrolysis phase ($OC3_{des/pyr}$ and $OC4_{des/pyr}$), as well as pyrogenic carbon ($OC1{-}3_{pyrogen}$). (B) Ratio of desorption/pyrolysis carbon to pyrogenic carbon according to the TOCA analysis deploying the common IMPROVE_A temperature protocol. PP asph ($n = 3$) and AA-Hep/Tol ($n = 2$) have been measured as replicates and included here to provide reproducibility information. Based on the PP asph triplicate measurement, a standard deviation of ∼0.1 can be assumed for the $OC_{des/pyr}$ to $OC_{pyrogen}$ ratio.

OC4 in helium (He) atmosphere and 580, 740, and 840 °C for EC1−EC3 in a 98 v-% He/2 v-% oxygen (O_2) atmosphere.[40] The released carbonaceous compounds are led through a heated oxidizer (manganese oxide at 900 °C) and are oxidized to carbon dioxide. Subsequently, a nondispersive infrared sensor (NDIR) detects and quantifies the carbon dioxide.[52] The signal is calibrated at the end of each experiment by 1 mL of a standard mixture of 5 v-% methane in helium. The following temperature step is not initiated until the NDIR signal stabilizes or reaches the baseline. Consequently the duration of each temperature step differs depending on the respective amount of carbon. The optical part of the TOCA includes a UV−vis-light source (seven modulated diode lasers with different wavelengths (405, 445, 532, 635, 780, 808, and 980 nm) and two detectors, one to measure the reflectance and one for the transmission. This optical measurement is required for the correction of organic and elemental carbon.[39,41] Between each measurement, the oven of the TOCA was heated for at least 10 min to 800 °C, preventing carry-over and memory effects.

Replicative measurements of the PP asphaltene reveal that the reproducibility of the TOCA measurements of the different carbon fractions depends exponentially on the absolute abundance (Figure S1). Fractions with a contribution below 5% revealed a standard variation of almost 100%, whereas fractions with contributions above 10% only varied about 3−10%, respectively. Generally, for the summed fractions of $OC_{des/pyr}$ and $OC_{pyrogen}$, a higher reproducibility was found with deviations between 6 and 8%.

High-Resolution Mass Spectrometry Evolved Gas Analysis. Roughly 8 v-% of the evolved gas mixture released from the stepwise heating of the sample material is transferred to mass spectrometric analysis via a heated hyphenation unit and transfer line (Figure 1). For this purpose, the quartz tube of the TOCA is modified to include a side arm with an outer diameter of one-eighth inch. Through this side arm, a deactivated fused silica capillary (inner diameter, 250 μm; length, 9 m) is guided for sampling. The entire transfer and hyphenation unit is heated to 250 °C, preventing recondensation. A recently introduced vacuum photoionization Orbitrap high-resolution mass spectrometer platform[47] was utilized for evolved gas analysis. Here, vacuum resonance-enhanced multiphoton ionization (REMPI) is realized inside the C-trap directly prior to injection into the Orbitrap mass analyzer. For this purpose, a PhotonEx (Photonion GmbH) Krypton-Fluoride excimer laser with a wavelength of 248 nm at an output energy of 192 μJ is used. Mass spectrometric data were recorded from m/z 50−750 with a repetition rate of approximately 2 Hz (512 ms Orbitrap transient length) achieving a resolving power of over 140,000 at m/z 200.

Data Analysis. The time-resolved data from the TOCA are exported to a comma-separated value spreadsheet format and imported to MATLAB (MATLAB R2020b) for further processing and visualization. The time- and temperature-resolved mass spectra from the Orbitrap mass spectrometer were recorded in two parallel and independent approaches: (1) standard built-in hardware and software (Thermo-Fisher Scientific, Software: Version 2.9 SP2 Build, Role: Factory) and (2) via an adapted external high-performance data acquisition (DAQ) system (FTMS Booster X2, Spectroswiss, Lausanne, Switzerland). The external DAQ system allowed for direct access to the unreduced time-domain data and enabled mass spectra representation in an absorption-mode FT (aFT). The latter is realized by combining in-hardware transient phasing performed with the FTMS Booster X2 digital signal processing module and allied data processing software (Peak-by-Peak Base Edition, version 2020.9.0, Spectroswiss). Elemental compositions were attributed scan-by-scan by a custom MATLAB user interface, named CERES, using the following boundaries: error width, 2 ppm; elemental composition, $C_{1-100}H_{1-200}N_{0-3}O_{0-5}S_{0-2}$.

RESULTS AND DISCUSSION

Asphaltene Thermal-Optical Carbon Analyzer Response. In this section, the results of the thermal-optical carbon analysis will be discussed. The applied IMPROVE_A protocol is a frequently used TOCA heating protocol. Generally, it differentiates into desorption steps (inert atmosphere, OC1 and OC2, < 280 °C), pyrolysis phases (inert atmosphere, OC3 and OC4, > 480 °C), as well as elemental carbon (oxidative atmosphere, EC1−3, > 580 °C). The literature has also shown its suitability for the analysis of engine fuels, which were compared to the respective primary combustion aerosol. Hence, this general applicability to fossil petroleum matrixes directly links to the presented work. Even though the terminology "elemental carbon" is a parametric definition based on the measurement concept of the TOCA, we use another denotation in this study: in contrast to particulate matter analysis, where ash and soot can be present, we hypothesize that no or a neglectable amount of soot is initially existing in the investigated asphaltene and crude oil samples. Consequently, the registration of elemental carbon is entirely caused by coking and charring processes during the OC temperature steps at an inert gas atmosphere and elevated temperature. Coking processes during thermal treatment in an inert atmosphere are the core principle of using the TOCA as a descriptor for asphaltene molecular architecture as this behavior was shown to be strongly structure-dependent.[27,53,54] Hence, based on this assumption, we will refer to this elemental carbon evidenced in EC1−3 as pyrogenic organic

https://doi.org/10.1021/acs.energyfuels.2c02122
Energy Fuels 2022, 36, 10177−10190

carbon ($OC_{pyrogen}$), whereas the fractions OC1−4 are referred to as desorption and pyrolysis organic carbon ($OC_{des/pyr}$).

Figure 2A summarizes the quantified relative response of the individual carbon fractions for the petroleum and asphaltene materials, whereas Figure 2B gives the ratio of $OC_{des/pyr}$ to $OC_{pyrogen}$. This ratio is commonly used in carbonaceous aerosol analysis for a more general description and classification of the complex material,[55,56] and advantageously random absolute errors do not affect this measure. An overview on the summed fractions can be found in Figure S2. For the PP crude oil, these bulk property insights reveal an almost equal distribution and relative contribution for the $OC1-3_{des/pyro}$ fraction, whereas the highest $OC4_{des/pyro}$ fraction at 580 °C was quantified with less than 1%. As the $OC_{des/pyro}$ steps of the TOCA thermal protocol are to some degree comparable to a classical distillation, the findings for the crude oil are expected. Interestingly, a relative contribution of almost 20% could be found for the first $OC_{pyrogen}$ step. This finding is linked to species undergoing coking reactions, most likely high-molecular weight, highly aromatic constituents, such as asphaltenes.

For the asphaltenes, Figure 2A immediately reveals that the island-enriched Wyoming asphaltene samples[15,33] and their corresponding extrographic fractions are the only samples showing a substantial contribution of the $OC2_{pyrogen}$ fraction. This finding is valuable evidence for the increased coking degree directly detected by the TOCA setup. The higher contribution of pyrogenic organic carbon can also be expressed by the ratio of $OC_{des/pyr}$ to $OC_{pyrogen}$ given in Figure 2B. Here, the single-core island-enriched Wyoming samples revealed very low ratios of 0.3−0.6, whereas the samples described as multi-core archipelago-enriched (Athabasca asphaltene and its extrographic fractions) revealed ratios of 0.8−1.9. These findings agree with the results from a previous study, where we found substantially higher thermogravimetric residues for island-rich asphaltenes compared to archipelago-enriched asphaltenes.[15] Interestingly, regarding the fraction distribution and the $OC_{des/pyr}$ to $OC_{pyrogen}$ ratio, the PetroPhase 2017 asphaltenes seem to be more similar to archipelago-enriched asphaltenes than to island-enriched samples. This finding is consistent with the literature, which described a higher proportion of archipelago species for the PetroPhase 2017 asphaltene, e.g., by IRMPD,[32] or thermal analysis mass spectrometry.[36] Furthermore, NMR was able to show the presence of archipelago species for several *n*-heptane asphaltenes.[53] The $OC3_{pyrogen}$ fraction (highest temperature elemental carbon step) was determined below <1% in relative contribution or not detectable for almost all samples except the Wyoming acetone fraction with a very low relative contribution of ∼1.3%. Also in aerosol science, where sample materials with high soot content are investigated, this fraction is rarely found and sparsely expressed.[45,46]

With increasing carbon number of the alkane solvent (C_5, C_6, and C_7) used for the precipitation, the ratio between $OC_{des/pyr}$ and $OC_{pyrogen}$ successively decreases as expected (Figure 2A,B).[57,58] This observation can be explained by a decreasing content of coprecipitated maltenes during the preparation process. Previously, we investigated the exact same sample materials with thermal analysis mass spectrometry and also found a higher contribution of codeposited maltenes for the smaller alkane solvents ($C_5 > C_6 > C_7$), which is in agreement with the solvent physicochemical properties, such as polarity and hydrophobicity. Thus, the TOCA allows not only an assessment of the bulk molecular architecture of the asphaltenes but also an insight into occluded maltene species. It is critical to highlight that this feature can also be a disadvantage as such contaminations might influence the response, e.g., resins occluded on the asphaltenes will increase the ratio by increasing the $OC_{des/pyr}$ relative contribution. In agreement with this concept, the crude oil, composed of dominantly maltenes and only a single-digit percentage of asphaltenes, revealed the highest ratio of 5.2. A simple scatter visualization of the $OC_{des/pyr}$ versus the $OC_{pyrogen}$ relative contributions in Figure 3 nicely depicts and summarizes the

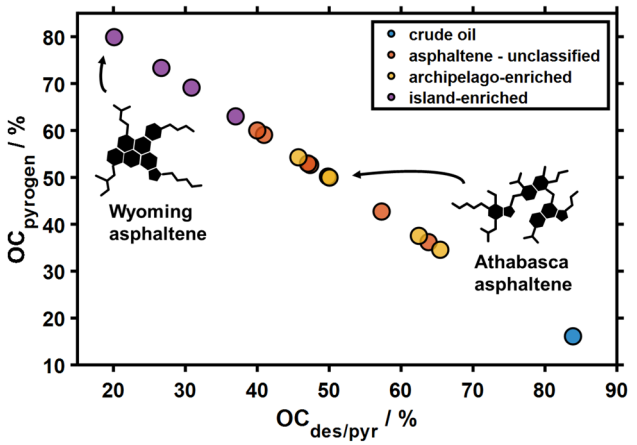

Figure 3. Scatter visualization of the $OC_{des/pyr}$ and $OC_{pyrogen}$ relative contributions. Color-coding according to the classification into crude oil (blue), unclassified - unknown enriched structure (red), archipelago multi-core enriched (yellow), and single-core island enriched (violet).

outlined behavior. Naturally, a linear relation is found, which quickly allows to see the characteristic grouping and differentiation capability by color-coding according to the classification into crude oil, unclassified (enriched asphaltene motif unknown), single- and multi-core asphaltenes.

It was shown that the extrographic fractionation of asphaltenes overcomes certain limitations of current analytical techniques, such as combating ionization suppression and matrix effects in mass spectrometry.[22,32,34] Thus, despite being very time- and labor-consuming, extensive extrographic fractionation provides a broader molecular insight with better coverage of the chemical/structural space. Consequently, the extrographic fractions of the Wyoming and Athabasca asphaltene partially revealed TOCA profiles enormously different from the whole asphaltene material. However, the lessons learned in mass spectrometry[22,32,33] on those fractions cannot be directly transferred to the TOCA results. The acetone fraction disrupts dipolar interactions and, thus, favors single-core island species as well as petroporphyrins. In direct infusion atmospheric pressure ionization with a higher ionization yield for island species, this fraction is commonly more similar to the whole asphaltene. Interestingly, for the quantified and less biased TOCA results, we found a higher contribution of $OC_{des/pyr}$ compared to the whole material. The heptane/toluene fraction, favoring less polar compounds, such as alkyl-aromatics, revealed a response close to the unfractionated sample. For the toluene/THF/methanol fraction, disrupting hydrogen bonds and favoring multi-core species, and for the acetone fraction, significantly lower

https://doi.org/10.1021/acs.energyfuels.2c02122
Energy Fuels 2022, 36, 10177−10190

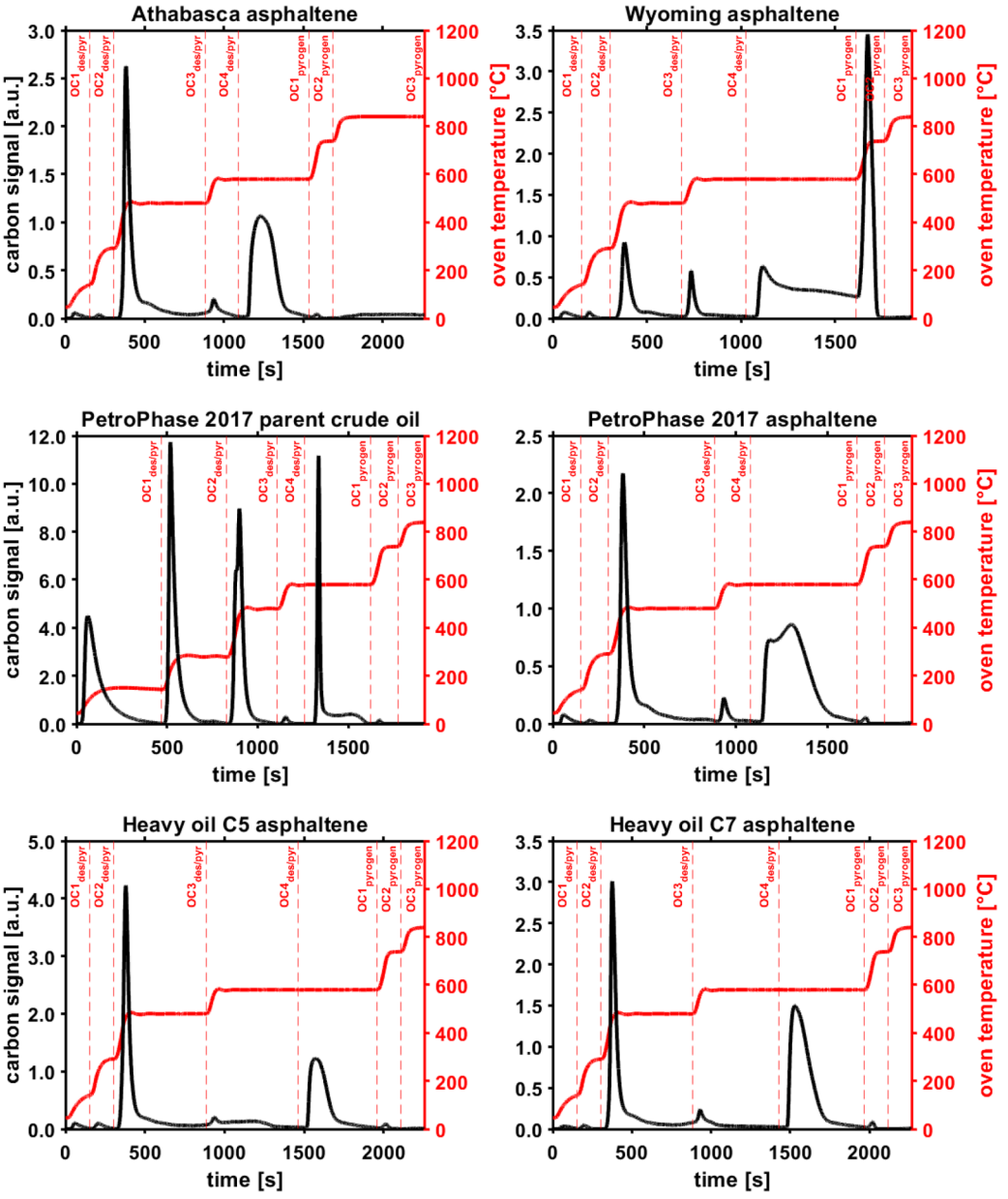

Figure 4. Time-resolved thermal-optical carbon analyzer response (quantitative carbon signal based on the carbon dioxide NDIR measurement) for the PetroPhase crude oil and corresponding asphaltene, the heavy oil C5 and C7 asphaltene as well as for the Athabasca bitumen and Wyoming deposit asphaltene. All time-traces can be found in the Supporting Information, Figures S3 and S4.

contributions of pyrogenic organic carbon were found. Particularly for the single-core-enriched Wyoming asphaltene, a higher contribution for $OC_{des/pyr}$ can be found in the extrographic fractions. Despite the quantification of the released carbon by the TOCA approach, a complex response, not just linked to the solvent properties, can be found. As hypothesized in a previous study with thermal analysis mass spectrometry, this effect might be explained by cooperative aggregation of occluded maltenes strongly bound to the asphaltenes.[59] This theory is supported by a higher $OC_{des/pyr}$ contribution for all extrographic fractions compared to the whole asphaltene samples, which show an increased $OC_{pyrogen}$ contribution.[15] Therefore, the extrographic fractionation does not only overcome selective ionization in mass spectrometry but also significantly affects intermolecular bonding[59] and, thus, the molecular information investigated by evolved gas analysis, which is later discussed in more detail for the mass spectrometric analysis.

The TOCA registers the evolved and quantified carbon with a frequency of roughly 1 Hz, which allows for temperature-resolved tracking of the emission profile. Figure 4 displays selected thermograms (traces for all samples can be found in the Supporting Information in Figures S3 and S4). It must be noted, that the IMPROVE_A protocol is a data-dependent temperature protocol; thus, the individual length of the steps varies with the sample material and amount. Nonetheless, the fraction set-temperature, heating rates, and atmosphere settings remain the same.

For the PP crude oil, rather sharp emission peaks are observed, distinctly different in abundance pattern and shape to the asphaltene profiles. The crude oil is dominated by high abundant peaks in the $OC1-3_{des/pyr}$ fraction as well as in the

https://doi.org/10.1021/acs.energyfuels.2c02122
Energy Fuels 2022, 36, 10177−10190

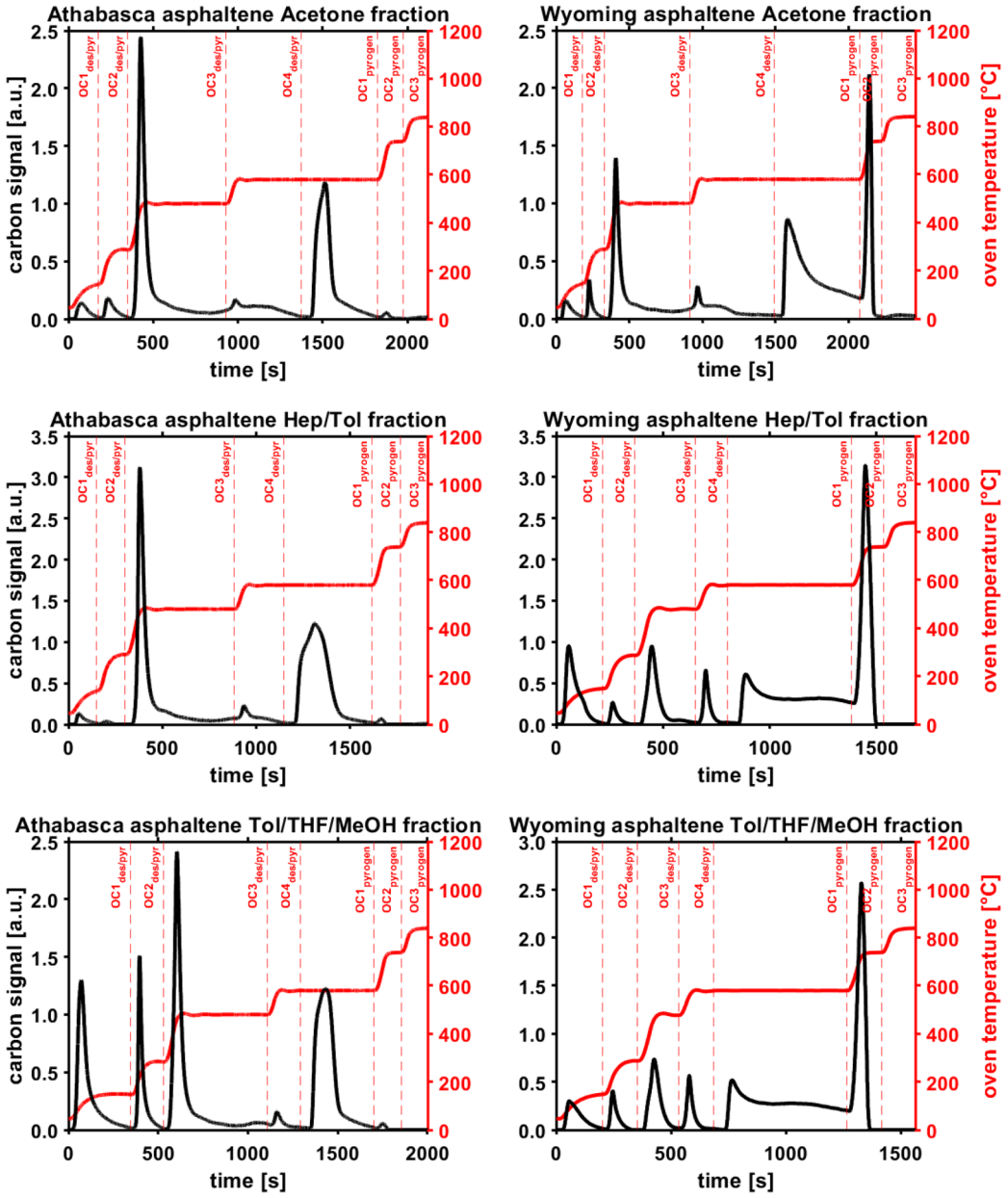

Figure 5. Time-resolved thermal-optical carbon analyzer response (quantitative carbon signal based on the carbon dioxide NDIR measurement) for the extrographic fractions of the Athabasca bitumen and Wyoming deposit asphaltene. All time-traces can be found in the Supporting Information, Figures S3 and S4.

$OC1_{pyrogen}$ fraction, whereas asphaltenes reveal a signal in the $OC3{-}4_{des/pyr}$ and $OC1_{pyrogen}$ fraction or $OC1{-}2_{pyrogen}$ fraction, respectively. In comparison to the crude oil, the $OC_{des/pyr}$ emission peaks of the asphaltenes show slightly stronger tailing, which may occur due to the enrichment in heteroatom-containing species with high aromaticity. For the $OC1_{pyrogen}$, there is still a peak-shaped response but with a much broader profile up to a strong plateauing effect. This delay in carbon response and the longer combustion reaction times could be explained by resistive structural moieties, which are harder to volatilize, even at elevated temperatures under an oxidative atmosphere.

Not only the crude oil reveals distinct differences to the asphaltenes but also the asphaltenes partially exhibit great differences in their emission profiles. The emission profile of the PetroPhase 2017 asphaltene shows a similar behavior to the archipelago-enriched Athabasca asphaltenes, whereas the profile of the island-enriched Wyoming asphaltenes differs significantly. The emission profiles for the $OC_{des/pyr}$ fractions are similarly shaped but differ in abundance and peak area for the different asphaltenes. For the single-core asphaltenes, the $OC1_{pyrogen}$ fraction occurs without a clear peak shape and strong plateau character. The occurrence of such a plateau is supported by the hypothesis of combustion-resistive coke formed during the pyrolysis under an inert atmosphere in the previous $OC_{des/pyr}$ fractions (up to 580 °C), which seem to have a strong structure dependency. These more-resistive coke species, predominantly observed for the single-core-enriched materials, are finally vaporized during even higher temperatures of 740 °C. Hence, as a unique behavior for those island-type dominated materials, the $OC2_{pyrogen}$ fraction occurs as a sharp, high abundant response. As explanation for these observations

https://doi.org/10.1021/acs.energyfuels.2c02122
Energy Fuels 2022, 36, 10177−10190

in the $OC2_{pyrogen}$ fractions, we hypothesize different coking mechanisms for island- and archipelago-type asphaltenes. In delayed coking, different forms of coke, especially shot coke (unreactive, low porosity, high density coke) and sponge coke (porous, disordered, highly cross-linked amorphous, or isotropic coke) are known.[53,60] Siskin and co-workers deeply investigated the coking behavior of a variety of asphaltenes and found that asphaltenes with more than one heteroatom per core unit favor the formation of shot coke, whereas asphaltenes with low heteroatom content per aromatic core favor the formation of sponge coke.[53,61,62] Based on this knowledge, we hypothesize that archipelago-type asphaltenes, which are composed of several smaller aromatic cores containing most likely only one heteroatom per core on average, form more porous sponge-like coke combustible during the $OC1_{pyrogen}$ fraction. Island-type asphaltenes seem to produce a more stable, shot-like coke due to their larger aromatic cores, which can contain several heteroatoms. Moreover, island-type molecules might be efficiently converted into relatively stable and resistive coke species with even higher aromaticity by the cleavage of alkyl-side chains and intramolecular rearrangements.

As outlined above, the complex interactions between resins, aromatics, saturates, and asphaltenes in crude oil contribute to charring and, therefore, to the response in the pyrogenic organic carbon fractions. Saturates are predominantly evaporated intact or with minimal char formation, whereas for the more polar resins and aromatics a higher tendency for thermal decomposition but also some degree of char formation has been reported.[63−65] These findings are in agreement with the TOCA temporal behavior of the different nonpurified heavy oil asphaltenes. Here, an enrichment of multi-core species can be concluded but also a strong impact of coprecipitated maltene species.

With regard to the extrographic fractions, the further separation and fractionation of the whole asphaltene significantly influences mass spectrometric results, due to the overcoming of selective ionization, but also the response of less biased approaches, such as thermogravimetric pyrolysis yield and TOCA response, is affected. Interestingly, the discussed overcoming of cooperative aggregation effects, seen for the relative OC fraction distribution, can even be better visualized based on the time-response (Figure 5 and Figure S4). In strong contrast to the whole sample, sharp emission profiles for the $OC1_{des/pyr}$ and $OC2_{des/pyr}$ steps can be registered for the extrographic fractions, especially for the Athabasca Tol/THF/MeOH fraction as well all Wyoming asphaltene fractions. Generally, it can be hypothesized that charring might be less pronounced for the extrographic fractions compared to the whole sample due to weaker aggregation effects.

To conclude this section, the quantified relative distribution of the desorption/pyrolysis organic carbon and the pyrogenic organic carbon can be used as a simplified classification for asphaltene molecular architecture. Moreover, the time-resolved profiles might even allow for hypothesizing on occlusion effects, coke formation potential, and coke formation pathways, schematically summarized in Figure 6. Particularly for samples with a substantial amount of coprecipitated maltenes, charring pathways are even more complex.

Mass Spectrometric Evolved Gas Analysis. This section discusses the molecular level speciation of the complex evolved gas mixtures released by the TOCA. First of all, some restrictions to this analysis will be given. The evolved gas

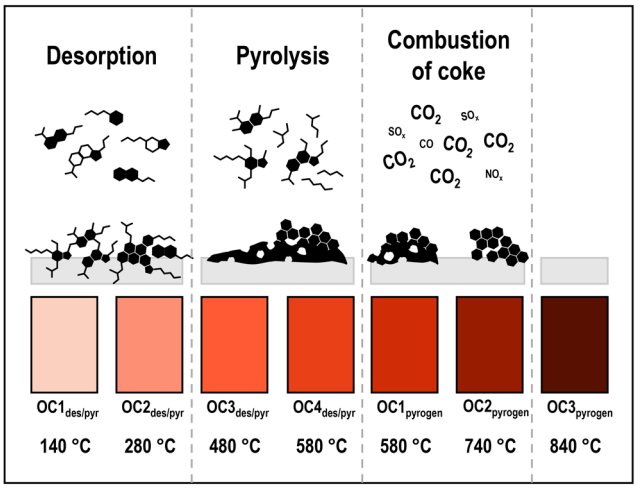

Figure 6. Schematic conclusion of thermal-optical carbon analysis of asphaltenes. The stepwise increase of the temperature leads to the evaporation of intact species at lower temperatures and inert atmosphere ($OC1_{des/pyr}$ and $OC2_{des/pyr}$), whereas at elevated temperature pyrolysis processes dominate. During $OC3_{des/pyr}$ and $OC4_{des/pyr}$, thermal degradation causes the generation of shot/sponge coke due to structural-dependent charring effects. This residual is combusted after a switch to an oxidative atmosphere at elevated temperatures ($OC_{pyrogen}$), generating carbon dioxide and other small gases.

mixture is guided through a heated transfer line at 250 °C with a flow rate of a few milliliters per minute to prevent condensation effects. The high aromaticity and polarity of the asphaltene species will certainly induce a bias, and high molecular weight compounds with low vapor pressure are discriminated. In comparison, despite matrix effects or suppression phenomena, direct infusion atmospheric pressure ionization, such as atmospheric pressure photo ionization, might be advantageous for introducing those heavier constituents. As the analysis relies on thermal evaporation/desorption, as well as intended pyrolysis, smaller thermal fragments are of focus for the EGA. The deployed Orbitrap mass analyzer delivers a resolving power of roughly 140,000 at m/z 200. Hence, challenging mass spectrometric splits, such as the C_3/SH_4 3.4 mDa split commonly observed in *Petroleomics*,[1,28] can only be addressed up to a certain mass limit of approximately m/z 400 (depending on the abundance ratios of the respective species). Consequently, the focus of the analysis in this study on thermal degradation products and a limited mass and vapor pressure region suits the deployed mass analyzer platform. More importantly, the resonance-enhanced multiphoton ionization (REMPI) is a technique sensitive and selective toward aromatic constituents, further simplifying the addressed chemical space for Orbitrap-based high-resolution mass spectrometric description.

Figure 7 gives an exemplary survey view of the TOCA-HRMS analysis for the PetroPhase 2017 asphaltene limited to the time-space of the organic carbon fractions under an inert gas atmosphere. As expected, after the $OC_{des/pyr}$ steps and change to an oxidative atmosphere ($OC_{pyrogen}$ fractions), no mass spectrometric signal was observed (Figure S5). This phenomenon is caused by the combustion and oxidation of the sample material generating small gaseous species, predominantly carbon dioxide, which cannot be detected with the REMPI Orbitrap platform. Carbon dioxide and monoxide but also substantial amounts of nitroxides as well as sulfur dioxide,

https://doi.org/10.1021/acs.energyfuels.2c02122
Energy Fuels 2022, 36, 10177−10190

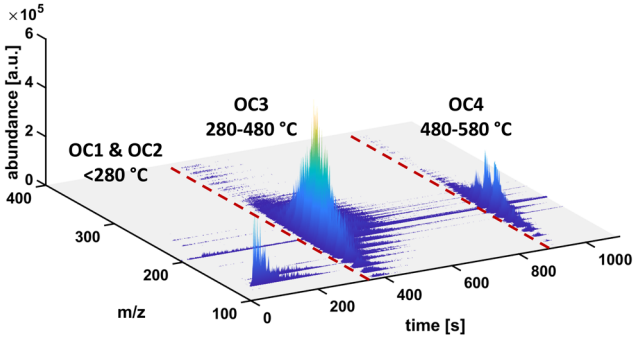

Figure 7. Exemplary survey view of the time-resolved high-resolution mass spectrometric response for the thermal-optical carbon analyzer evolved gas analysis for the PetroPhase 2017 asphaltene. Only few signals appear at desorption temperatures ($OC1_{des/pyr}$ and $OC2_{des/pyr}$), whereas a strong signal with a broad mass spectrometric range is registered at elevated pyrolysis temperatures ($OC3_{des/pyr}$ and $OC4_{des/pyr}$).

which are caused by the high heteroatom content of asphaltenes, will be released. Besides that, the release of alkenes, dienes, and other small organic thermal cleavage products, caused by the pyrolysis of side chains from the single- or multi-core compounds cannot be addressed here.[36] The focus is, however, on the molecular description of the evaporable aromatic cores. During the desorption phase (<280 °C) only a few signals can be detected with low complexity and more narrow mass range compared to the steps at elevated temperatures. This observation is strongly dependent on occluded maltenes and was found lowest for the Athabasca/Wyoming whole sample and for the PetroPhase2017 asphaltene (Figure 8, upper half) due to their high purification. At temperatures above 280 °C ($OC3_{des/pyr}$), a broad release pattern with CH_2−units (m/z 14) covering an m/z of 100 up above 350 can be observed (Figure 8, lower half). The second pyrolysis organic carbon fraction ($OC4_{des/pyr}$) at temperatures above 480 °C was found to be less complex. The extensive intended thermal fragmentation resulted in a shift toward lower masses. These findings directly agree with previous evolved gas analysis of asphaltene and heavy petroleum fractions conducted on an ultrahigh-resolution Fourier-transform ion cyclotron resonance mass spectrometer.[15,36]

As $OC1_{des/pyr}$ and $OC2_{des/pyr}$ (140 and 280 °C) generally causing evaporation processes, whereas $OC3_{des/pyr}$ and $OC4_{des/pyr}$ (480 and 580 °C) induce extensive pyrolysis, the data are combined for these two cases, respectively. Generally, based on the elemental composition attribution, the evolved chemistry is strongly dominated by CH-class compounds with high double bond equivalents (DBEs), structurally attributed to alkylated series and core structures of polycyclic aromatic hydrocarbons (PAHs). The contribution of CHS-, CHO-, and CHN-class compounds is an order of magnitude lower. Despite low ion suppression and negligible matrix effects, also in vacuum photoionization, the ion yield (ionization cross section) will primarily be affected by the respective structure of the analyte. REMPI delivers high ionization cross sections and, thus, excellent sensitivities for PAH cores, such as phenanthrene, pyrene, or benz[*a*]pyrene. In contrast, polycyclic aromatic sulfur-containing heterocycles (PASH) are generally ionized with orders of magnitude lower cross-section. Hence, PAHs might be overrepresented in the EGA by the REMPI spectrum.

In the $OC1_{des/pyr}$ and $OC2_{des/pyr}$ fraction, frequently, C_7H_7 (tropylium cation based on toluene), C_7H_8 (toluene), $C_{10}H_8$ (naphthalene), $C_{11}H_{10}$ (methyl-naphthalene), $C_{12}H_{12}$ (dimethyl/ethyl-naphthalene), and traces of $C_{14}H_{10}$ (phenanthrene/anthracene) as well as $C_{16}H_{10}$ (pyrene/fluoranthene) can be detected for almost all samples. These small aromatics are most likely occluded species from the aromatic fraction, non-covalently strongly bound based on $\pi-\pi$-electron interactions. Released in trace amounts, these species are detected in the aromatic sensitive and selective REMPI analysis. However, as also purified asphaltenes exhibit these signals, a certain contribution could also be caused by contamination or carry-over effects. The PP crude oil exhibits an expected profile of alkylated series of two- to four-ring PAHs between m/z 150−300, centered at around m/z 200. Interestingly, the Tol/THF/MeOH extrographic fraction of the Wyoming asphaltene exhibits additional aromatic small molecules ($<m/z$ 200) (Figure S6). This finding is in agreement with TG-APCI-FT-ICR MS data on the same sample materials.[15] Here, particularly the acetone and Tol/THF/MeOH extrographic fractions have shown a strong mass spectrometric response for the desorption phase (<350 °C). APCI has particularly found CH, CHO_1, and CHO_2 species close to the planar aromatic limit. We suggest that the performed analyses are highly consistent, given the selectivity of REMPI for CH-class PAH compounds. For the acetone fraction, APCI showed a stronger contribution of less aromatic, higher molecular weight and more polar species. Contradictory, in this study, no substantial additional signals, except small aromatic species, could be detected. We hypothesize that this effect could be caused by the REMPI ionization selectivity and the prototype heated transfer into the mass spectrometer, which could preclude the detection of these occluded constituents.

For the averaged mass spectrometric response of $OC3_{des/pyr}$ and $OC4_{des/pyr}$, the archipelago-enriched Athabasca asphaltene samples generally exhibit a broader emission profile covering a wider mass range and longer alkylated series. In contrast, the Wyoming asphaltene samples enriched in single-core island species revealed a narrower pattern at a lower m/z. Regarding the overall complexity, a significantly higher number of attributed elemental compositions could be found for the Athabasca asphaltene and its extrographic fractions (873−1287) compared to the Wyoming asphaltene and respective extrographic fractions (353−574). This finding is in agreement with the overall lower complexity depicted from the mass spectra (Figure 8 and Figure S7), most likely caused by the substantial proportion of charring and coking of the island-enriched materials with less options for aromatic thermally evaporable cleavage products detectable by REMPI. For the PetroPhase 2017 asphaltene, a mass spectrometrc complexity in-between the single- and multi-core-enriched materials has been found (A 882, W 424, PP asph 593). This could be caused by a more equally distributed molecular architecture of the PP asph with a tendency toward multi-core constituents. The three heavy oil asphaltenes differing in precipitation solvent (HO8C5−C7) show no significant differences for the mass spectrometric profile of the $OC3_{des/pyr}$ and $OC4_{des/pyr}$ fractions. Based on the effect of the *n*-alkanes on the precipitation, studied during decades in numerous work, this finding is expected.[57,58,66] The high molecular weight asphaltene fraction is similarly present in all of the three samples and, thus, similar pyrolytic fragments could be observed. This observation was previously reported on the

https://doi.org/10.1021/acs.energyfuels.2c02122
Energy Fuels 2022, 36, 10177−10190

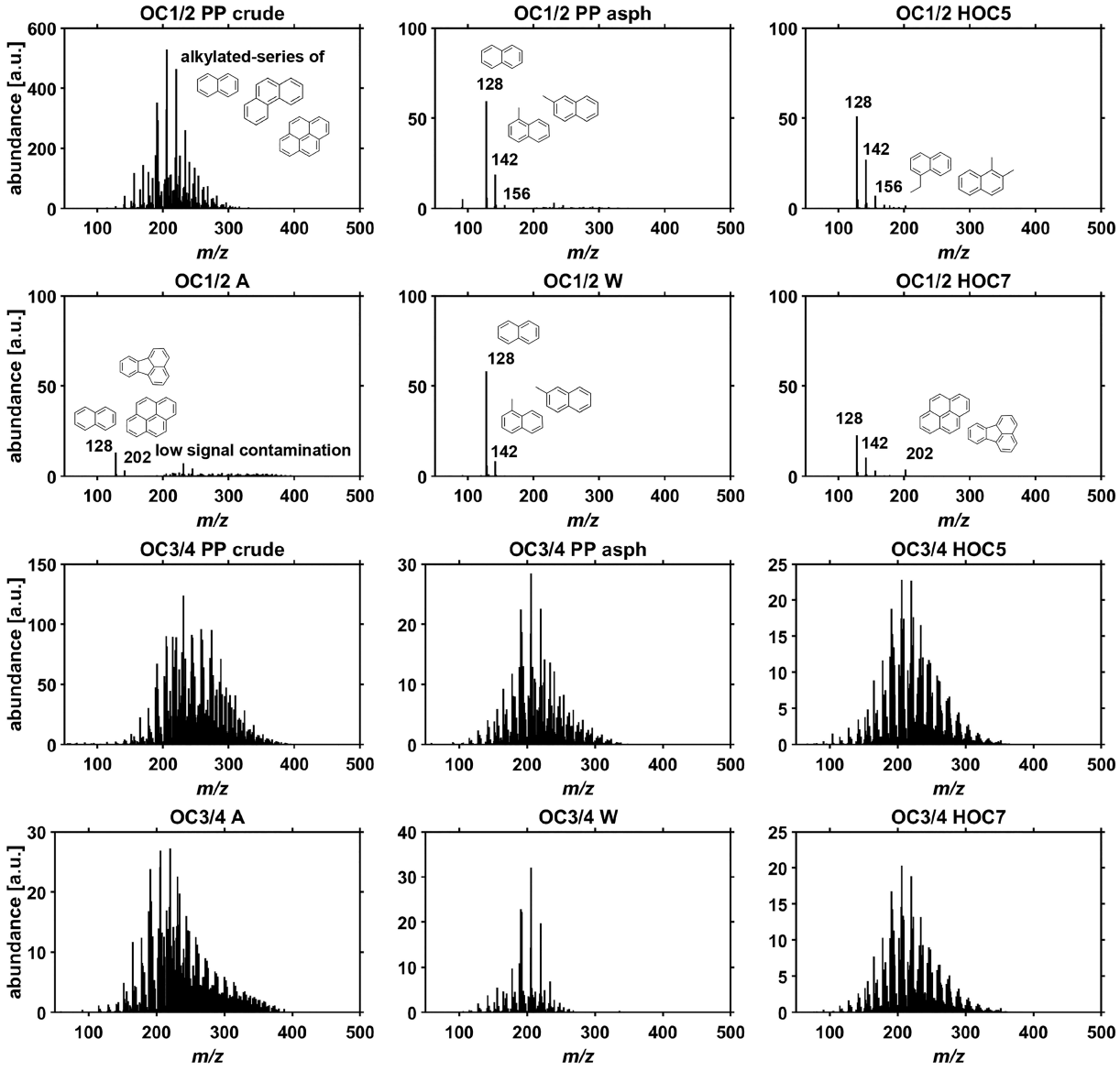

Figure 8. Average resonance-enhanced multiphoton ionization Orbitrap high-resolution mass spectra of $OC1_{des/pyr}$ and $OC2_{des/pyr}$ (140/280 °C) and $OC3_{des/pyr}$ and $OC4_{des/pyr}$ (480/580 °C) fractions for the PetroPhase crude oil and corresponding asphaltene, the heavy oil C5 and C7 asphaltene as well as for the Athabasca bitumen and Wyoming deposit asphaltene.

same sample set deploying thermogravimetry coupled to APCI FT-ICR MS.[34] However, the samples differ in the amount of coprecipitated maltenes evaporated at lower temperatures, presumable not or poorly detectable via REMPI-MS.

With respect to the chemistry of the attributed formulas, the CH-class largely dominates and accounts for 65−85% of the overall detected mass spectrometric response. However, CHS-, CHO-, and CHN-class constituents have been detected with relative abundances between 6 and 16%. Here, particularly the acetone extrographic fraction of both, the Wyoming and Athabasca asphaltene, attracts attention with the highest contribution of heteroatom-containing species. This result confirms the higher polar character of the acetone fraction, partially covered by the accessible chemical space of the REMPI. The primary differences found in the alkylation length and pattern can be depicted from the carbon number versus DBE diagrams given in Figure 9. Here, only the radical cations (odd electron configuration) of the dominant CH-class are depicted. Carbon number histograms are supplied in Figure S9. At first sight, all distributions appear very similar and can be found close to the planar aromatic limit with slopes close to one characteristic for asphaltenes,[67] which corresponds to condensed aromatic PAHs released during the thermal degradation in $OC3_{des/pyr}$ and $OC4_{des/pyr}$. However, comparing the alkylation length of the distribution, distinct differences between the asphaltene samples can be concluded. All asphaltenes reported with an enrichment of multi-core constituents reveal longer/a higher number of alkylation side chains. In contrast, the asphaltenes described as enriched in single-core species exhibit a shorter alkylation length/number. This observation can also be made from other compound classes, such as the CHS_1-class (Figure S8). Compared to our previous work on thermal analysis mass spectrometry of asphaltenes, these results must be placed in context.[15] In TG-APCI FT-ICR MS, two DBE/#C distribution patterns characteristic for single-core constituents have been reported:

https://doi.org/10.1021/acs.energyfuels.2c02122
Energy Fuels 2022, 36, 10177−10190

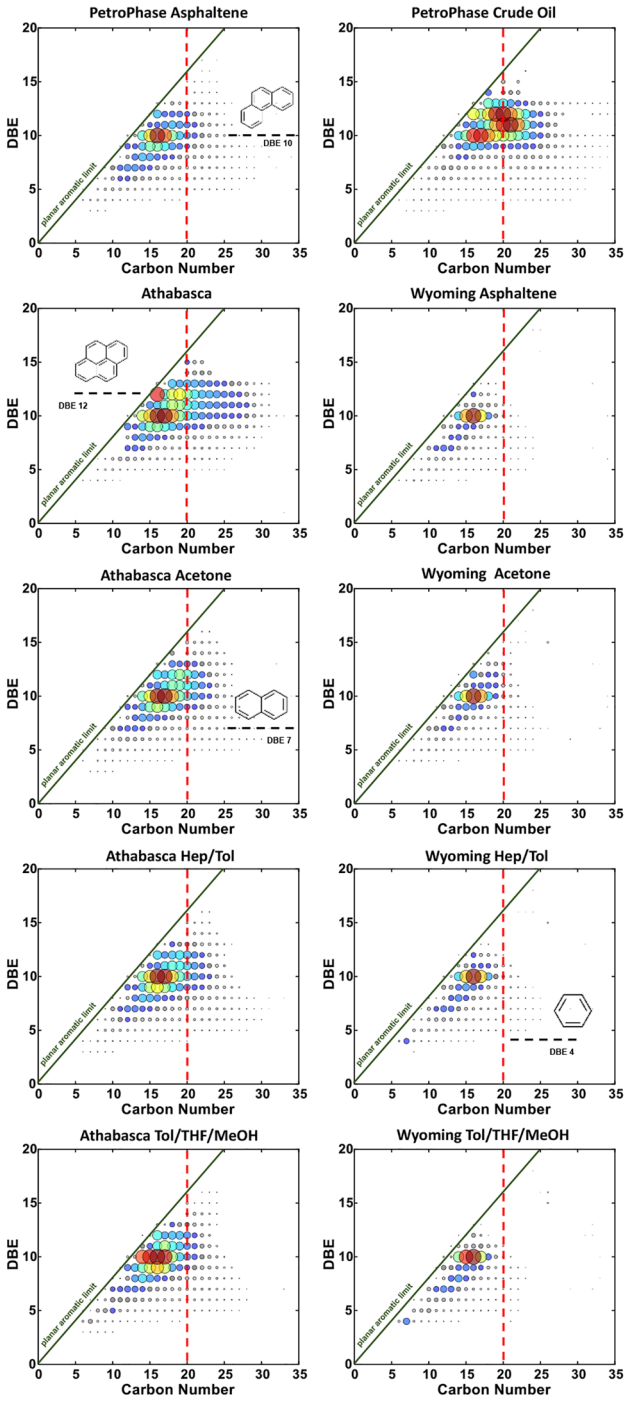

Figure 9. Double bond equivalent (DBE) versus carbon number representation of the average OC3 $_{des/pyr}$ and OC4$_{des/pyr}$ (480/580 °C) fractions for the PetroPhase asphaltene and crude oil, as well as the Athabasca and Wyoming asphaltene with their respective extrographic fractions for the dominating CH-class (odd electron configuration, radical cations). The planar aromatic limit is given in green. Selected prominent alkylated DBE rows are tentatively labeled with plausible PAH core structures. A dashed vertically red line at carbon number 20 is given for simpler pattern comparison.

one close to the planar aromatic limit with low carbon numbers and a second at low DBE values with broad carbon number spread. Taking REMPI with selectivity for aromatic species (DBE > 3) into account, solely the first pattern can be found and confirmed for the island structures. Moreover, also the characteristic pattern for archipelago structures found for the APCI analysis at moderate DBE values with broader carbon number spread and higher alkylation length can be confirmed here to some extent. Nonetheless, high ionization cross sections for the PAHs and limited thermal transfer and sampling most likely shift the observed REMPI pattern for the multi-core pyrolysis products closer to the planar aromatic limit, making it more similar to the molecular pattern revealed by the thermal degradation of the single-core-enriched samples.

The high similarity of the respective extrographic fractions of the Wyoming and Athabasca asphaltene can be explained by the predominant measurement of asphaltene species in OC3$_{des/pyr}$ and OC4$_{des/pyr}$ with a lower contribution of occluded maltene species or aggregation effects discussed above. Moreover, the found differentiation in alkylation length can also be expressed by an average alkylation number based on the PAH core structure at the planar aromatic limit. Basically, this measure calculates alkylation length for each DBE value starting at the lowest carbon number given by the planar aromatic limit line (DBE = 0.8 × #C), e.g., for DBE 7 (naphthalene), the carbon number starting point would be #C 9. This calculation confirms the visual findings from the DBE versus carbon number plots. It results in a higher average alkylation length for the asphaltene samples dominated by multi-core species (A, 5.8; A-Ace, 5.14; A-Hep/Tol, 5.3; A-Tol/THF/MeOH, 4.52) compared to the samples enriched in single-core species (W, 3.71; W-Ace, 3.84; W-Hep/Tol, 3.9; W-Tol/THF/MeOH, 3.59). For the PP asph, a value (4.97) in between but with a tendency toward the archipelago-enriched samples can be found. Even though the differences in the intensity-weighted alkylation length are low, they might be used as a support for the classification approach. However, the effects are not as pronounced as for other mass spectrometric studies[15,22] and significantly less striking than the TOCA response discussed above in this work.

CONCLUSION

In the framework of asphaltene structural elucidation, a thermal-/optical carbon analyzer hyphenated to an Orbitrap mass spectrometer was deployed for the analysis of various asphaltene materials, an asphaltene parent crude oil, as well as extrographic asphaltene fractions. Previous thermogravimetric analysis could only trace the mass loss along with the thermal treatment. Hence, primarily, the capability of the TOCA for a temperature-resolved quantification of the released carbon is used together with the option of applying an inert or oxidative atmosphere. Based on the investigation of samples described either enriched in single- or multi-core constituents, we could successfully show that the relative proportion of OC$_{des/pyro}$ and OC$_{pyrogen}$, as well as the ratio of OC$_{des/pyr}$/ OC$_{pyrogen}$, can be used as a classification approach for the prevalent molecular architecture. We hypothesize that this finding is caused by different coking and charring behavior strongly depending on the molecular architecture of single- and multi-core constituents. Here, island species will result in a lower evaporable fraction and more resistive char detected later during the OC$_{pyrogen}$ fractions. Conclusions on the occurrence of occluded maltenes as well as on overcoming aggregation effects could be taken. Generally, maltenic compounds tend to occur in the OC$_{des/pyro}$ phase and thus shift the OC$_{des/pyro}$/ OC$_{pyrogen}$ to higher values. For future investigations, e.g., on biomass pyrolysis residues or asphaltenes from recycling oils,

https://doi.org/10.1021/acs.energyfuels.2c02122
Energy Fuels 2022, 36, 10177−10190

particularly an adaption of the thermal analysis protocol with lower heating rates could be of interest. These further studies could try to unravel different charring pathways contributing to the formation of shot- and sponge-like coke.

Ionization of the evolved gas mixture by REMPI and subsequent Orbitrap mass analysis has revealed a strong selectivity and high sensitivity for the PAHs and allows for a molecular description of the complex pattern on the molecular level. Nonetheless, high ionization yields for these classical PAHs and low ionization cross sections for heteroatom-containing aromatic compounds partially disregard the asphaltene complexity. However, the alkylation pattern/length of the mass spectra received in $OC3_{des/pyr}$ and $OC4_{des/pyr}$ (480/580 °C) fractions have been identified as a classification measure with significantly lower and more narrow patterns for the asphaltenes dominated by single-core species.

We discussed the combination and necessity of different mass spectrometric platforms with multiple ionization schemes for the in-depth evolved gas analysis before.[36] Consequently, future studies will focus on the utilization of FT-ICR MS with atmospheric pressure ionization[15] for evolved gas analysis, deploying the TOCA as asphaltene molecular architecture classification concept. Moreover, further work will study the application of TOCA EGA-MS for other asphaltene and heavy residual materials, addressing research questions in the circular economy and recycling context. Additionally, the vacuum photo ionization Orbitrap mass spectrometer platform will be modified to realize other photo ionization schemes. In this respect, deuterium lamp-based single-photon ionization (SPI) and novel excimer VUV laser concept could be of interest.

■ ASSOCIATED CONTENT

Supporting Information

The Supporting Information is available free of charge at https://pubs.acs.org/doi/10.1021/acs.energyfuels.2c02122.

Table of overview on bulk data for selected asphaltene and heavy residue sample materials and figures of mean proportion versus relative standard deviation of a triplicate measurement of the PetroPhase C7 asphaltene, summed relative contributions for the $OC_{des/pyr}$ and $OC_{pyrogen}$ for all investigated sample materials, time-resolved thermal-optical carbon analyzer response (quantitative carbon signal based on the carbon dioxide NDIR measurement), total ion count chromatogram of the TOCA REMPI Orbitrap mass spectrometric analysis of the Athabasca a cetone sample, average resonance-enhance multiphoton ionization Orbitrap high-resolution mass spectrometry of $OC1_{des/pyr}$ and $OC2_{des/pyr}$ (140/280 °C) as well as $OC3_{des/pyr}$ and $OC4_{des/pyr}$ (480/580 °C) fractions, double bond equivalent (DBE) versus carbon number representation of the average $OC3_{des/pyr}$ and $OC4_{des/pyr}$ (480/580 °C) fractions, and stacked histograms of the carbon number distribution of the CH-, CHS_1-, CHN_1-, and CHO_1-class of the average $OC3_{des/pyr}$ and $OC4_{des/pyr}$ (480/580 °C) fractions (PDF)

■ AUTHOR INFORMATION

Corresponding Author

Christopher P. Rüger − *Joint Mass Spectrometry Centre (JMSC)/Chair of Analytical Chemistry, University of Rostock, 18059 Rostock, Germany; Department Life, Light & Matter (LLM), University of Rostock, 18059 Rostock, Germany; International Joint Laboratory−iC2MC: Complex Matrices Molecular Characterization, TRTG, 76700 Harfleur, France;* orcid.org/0000-0001-9634-9239; Email: christopher.rueger@uni-rostock.de

Authors

Anika Neumann − *Joint Mass Spectrometry Centre (JMSC)/Chair of Analytical Chemistry, University of Rostock, 18059 Rostock, Germany; Department Life, Light & Matter (LLM), University of Rostock, 18059 Rostock, Germany*

Paul Kösling − *Joint Mass Spectrometry Centre (JMSC)/Chair of Analytical Chemistry, University of Rostock, 18059 Rostock, Germany; Department Life, Light & Matter (LLM), University of Rostock, 18059 Rostock, Germany*

Silvia Juliana Vesga Martínez − *Joint Mass Spectrometry Centre (JMSC)/Chair of Analytical Chemistry, University of Rostock, 18059 Rostock, Germany; Department Life, Light & Matter (LLM), University of Rostock, 18059 Rostock, Germany*

Martha Liliana Chacón-Patiño − *International Joint Laboratory−iC2MC: Complex Matrices Molecular Characterization, TRTG, 76700 Harfleur, France; National High Magnetic Field Laboratory, Florida State University, Tallahassee, Florida 32310, United States;* orcid.org/0000-0002-7273-5343

Ryan P. Rodgers − *International Joint Laboratory−iC2MC: Complex Matrices Molecular Characterization, TRTG, 76700 Harfleur, France; National High Magnetic Field Laboratory, Florida State University, Tallahassee, Florida 32310, United States;* orcid.org/0000-0003-1302-2850

Ralf Zimmermann − *Joint Mass Spectrometry Centre (JMSC)/Chair of Analytical Chemistry, University of Rostock, 18059 Rostock, Germany; Department Life, Light & Matter (LLM), University of Rostock, 18059 Rostock, Germany; Joint Mass Spectrometry Centre, Cooperation Group "Comprehensive Molecular Analytics", Helmholtz Zentrum Muenchen, Neuherberg D-85764, Germany*

Complete contact information is available at: https://pubs.acs.org/10.1021/acs.energyfuels.2c02122

Notes

The authors declare no competing financial interest.

■ ACKNOWLEDGMENTS

This work was financed and supported by the EUROSTARS project E! 12083 "AerOrbi". Support by the Helmholtz International Lab. aeroHEALTH (www.aerohealth.eu) is gratefully acknowledged. The authors thank the Interdisciplinary Faculty, Department Life, Light and Matter of the University of Rostock for providing laboratory space and infrastructure. A portion of the work presented herein was performed at the National High Magnetic Field Laboratory ICR User Facility, which is supported by the National Science Foundation Division of Chemistry through Cooperative Agreement DMR-1644779, and the State of Florida.

■ REFERENCES

(1) Marshall, A. G.; Rodgers, R. P. Petroleomics: chemistry of the underworld. *Proc. Natl. Acad. Sci. U.S.A.* **2008**, *105* (47), 18090−18095.

(2) Palacio Lozano, D. C.; Thomas, M. J.; Jones, H. E.; Barrow, M. P. Petroleomics: Tools, Challenges, and Developments. *Annual Rev. Anal. Chem.* **2020**, *13* (1), 405−430.
(3) Rodgers, R. P.; McKenna, A. M. Petroleum analysis. *Analytical chemistry* **2011**, *83* (12), 4665−4687.
(4) Pandey, A.; Bhaskar, T.; Stöcker, M.; Sukumaran, R. K. *Recent advances in thermochemical conversion of biomass*; Elsevier, 2015.
(5) Bridgwater, A. V. Review of fast pyrolysis of biomass and product upgrading. *Biomass and Bioenergy* **2012**, *38*, 68−94.
(6) Palos, R.; Gutiérrez, A.; Vela, F. J.; Olazar, M.; Arandes, J. M.; Bilbao, J. Waste Refinery: The Valorization of Waste Plastics and End-of-Life Tires in Refinery Units. A Review. *Energy Fuels* **2021**, *35* (5), 3529−3557.
(7) Gray, N.; McDonagh, S.; O'Shea, R.; Smyth, B.; Murphy, J. D. Decarbonising ships, planes and trucks: An analysis of suitable low-carbon fuels for the maritime, aviation and haulage sectors. *Advances in Applied Energy* **2021**, *1*, 100008.
(8) Moud, A. A. Asphaltene induced changes in rheological properties: A review. *Fuel* **2022**, *316*, 123372.
(9) Alimohammadi, S.; Zendehboudi, S.; James, L. A comprehensive review of asphaltene deposition in petroleum reservoirs: Theory, challenges, and tips. *Fuel* **2019**, *252*, 753−791.
(10) Mohammed, I.; Mahmoud, M.; Al Shehri, D.; El-Husseiny, A.; Alade, O. Asphaltene precipitation and deposition: A critical review. *J. Pet. Sci. Eng.* **2021**, *197*, 107956.
(11) Adams, J. J. Asphaltene Adsorption, a Literature Review. *Energy Fuels* **2014**, *28* (5), 2831−2856.
(12) Furimsky, E. Deactivation of hydroprocessing catalysts. *Catal. Today* **1999**, *52* (4), 381−495.
(13) Akbarzadeh, K.; Hammami, A.; Kharrat, A.; Zhang, D.; Allenson, S.; Creek, J.; Kabir, S.; Jamaluddin, A. J.; Marshall, A. G.; Rodgers, R. P.; Mullins, O. C.; Solbakken, T. Asphaltenes—Problematic but Rich in Potential. *Oilfield Review* **2007**, 22−43.
(14) Zhang, Y.; Siskin, M.; Gray, M. R.; Walters, C. C.; Rodgers, R. P. Mechanisms of Asphaltene Aggregation: Puzzles and a New Hypothesis. *Energy Fuels* **2020**, *34* (8), 9094−9107.
(15) Neumann, A.; Chacón-Patiño, M. L.; Rodgers, R. P.; Rüger, C. P.; Zimmermann, R. Investigation of Island/Single-Core- and Archipelago/Multicore-Enriched Asphaltenes and Their Solubility Fractions by Thermal Analysis Coupled with High-Resolution Fourier Transform Ion Cyclotron Resonance Mass Spectrometry. *Energy Fuels* **2021**, *35* (5), 3808−3824.
(16) Chacón-Patiño, M. L.; Vesga-Martínez, S. J.; Blanco-Tirado, C.; Orrego-Ruiz, J. A.; Gómez-Escudero, A.; Combariza, M. Y. Exploring Occluded Compounds and Their Interactions with Asphaltene Networks Using High-Resolution Mass Spectrometry. *Energy Fuels* **2016**, *30* (6), 4550−4561.
(17) Saad, S.; Zeraati, A. S.; Roy, S.; Shahriar Rahman Saadi, M. A.; Radović, J. R.; Rajeev, A.; Miller, K. A.; Bhattacharyya, S.; Larter, S. R.; Natale, G.; Sundararaj, U.; Ajayan, P. M.; Rahman, M. M.; Kibria, M. G. Transformation of petroleum asphaltenes to carbon fibers. *Carbon* **2022**, *190*, 92−103.
(18) Enayat, S.; Tran, M. K.; Salpekar, D.; Kabbani, M. A.; Babu, G.; Ajayan, P. M.; Vargas, F. M. From crude oil production nuisance to promising energy storage material: Development of high-performance asphaltene-derived supercapacitors. *Fuel* **2020**, *263*, 116641.
(19) Qin, F.; Tian, X.; Guo, Z.; Shen, W. Asphaltene-Based Porous Carbon Nanosheet as Electrode for Supercapacitor. *ACS Sustainable Chem. Eng.* **2018**, *6* (11), 15708−15719.
(20) Ok, S.; Samuel, J. Obtaining Nanoporous Polycyclic Aromatic Hydrocarbon Networks by Cross-Linking Asphaltenes. *Energy Fuels* **2021**, *35* (13), 10937−10943.
(21) Siddiqui, M. N.; Pervez, S.; Karbhal, I.; Dugga, P.; Rajendran, S.; Pervez, Y. F. Using functionalized asphaltenes as effective adsorbents for the removal of chromium and lead metal ions from aqueous solution. *Environmental Research* **2022**, *204*, 112361.
(22) Chacón-Patiño, M. L.; Gray, M. R.; Rüger, C.; Smith, D. F.; Glattke, T. J.; Niles, S. F.; Neumann, A.; Weisbrod, C. R.; Yen, A.; McKenna, A. M.; Giusti, P.; Bouyssiere, B.; Barrère-Mangote, C.; Yarranton, H.; Hendrickson, C. L.; Marshall, A. G.; Rodgers, R. P. Lessons Learned from a Decade-Long Assessment of Asphaltenes by Ultrahigh-Resolution Mass Spectrometry and Implications for Complex Mixture Analysis. *Energy Fuels* **2021**, *35* (20), 16335−16376.
(23) Calemma, V.; Rausa, R. Thermal decomposition behaviour and structural characteristics of asphaltenes. *Journal of Analytical and Applied Pyrolysis* **1997**, *40*−*41*, 569−584.
(24) Strausz, O. P.; Mojelsky, T. W.; Faraji, F.; Lown, E. M.; Peng, P. Additional Structural Details on Athabasca Asphaltene and Their Ramifications. *Energy Fuels* **1999**, *13* (2), 207−227.
(25) Karimi, A.; Qian, K.; Olmstead, W. N.; Freund, H.; Yung, C.; Gray, M. R. Quantitative Evidence for Bridged Structures in Asphaltenes by Thin Film Pyrolysis. *Energy Fuels* **2011**, *25* (8), 3581−3589.
(26) Rueda-Velásquez, R. I.; Freund, H.; Qian, K.; Olmstead, W. N.; Gray, M. R. Characterization of Asphaltene Building Blocks by Cracking under Favorable Hydrogenation Conditions. *Energy Fuels* **2013**, *27* (4), 1817−1829.
(27) Gray, M. R.; Chacón-Patiño, M. L.; Rodgers, R. P. Structure-Reactivity Relationships for Petroleum Asphaltenes. *Energy Fuels* **2022**, *36* (8), 4370−4380.
(28) Rodgers, R. P.; Marshall, A. G. Petroleomics: Advanced Characterization of Petroleum-Derived Materials by Fourier Transform Ion Cyclotron Resonance Mass Spectrometry (FT-ICR MS). In *Asphaltenes, Heavy Oils, and Petroleomics*; Mullins, O. C., Sheu, E. Y., Hammami, A., Marshall, A. G., Eds.; Springer: New York, 2007; pp 63−93.
(29) Silva, L. C. d.; Dávila, J. V.; Fleming, F. P.; Combariza, M. Y.; Vaz, B. G. Laser desorption ionization and collision induced dissociastion as powerful tools for FT-ICR mass spectrometric characterization of asphaltene fractions enriched in island and archipelago motifs. *Fuel* **2022**, *323*, 124418.
(30) Thomas, M. J.; Jones, H. E.; Palacio Lozano, D. C.; Gavard, R.; Carney, S.; Barrow, M. P. Comprehensive analysis of multiple asphaltene fractions combining statistical analyses and novel visualization tools. *Fuel* **2021**, *291*, 120132.
(31) Chacón-Patiño, M. L.; Rowland, S. M.; Rodgers, R. P. Advances in Asphaltene Petroleomics. Part 1: Asphaltenes Are Composed of Abundant Island and Archipelago Structural Motifs. *Energy Fuels* **2017**, *31* (12), 13509−13518.
(32) Chacón-Patiño, M. L.; Rowland, S. M.; Rodgers, R. P. Advances in Asphaltene Petroleomics. Part 2: Selective Separation Method That Reveals Fractions Enriched in Island and Archipelago Structural Motifs by Mass Spectrometry. *Energy Fuels* **2018**, *32* (1), 314−328.
(33) Chacón-Patiño, M. L.; Rowland, S. M.; Rodgers, R. P. Advances in Asphaltene Petroleomics. Part 3. Dominance of Island or Archipelago Structural Motif Is Sample Dependent. *Energy Fuels* **2018**, *32* (9), 9106−9120.
(34) Rüger, C. P.; Neumann, A.; Sklorz, M.; Schwemer, T.; Zimmermann, R. Thermal Analysis Coupled to Ultrahigh Resolution Mass Spectrometry with Collision Induced Dissociation for Complex Petroleum Samples: Heavy Oil Composition and Asphaltene Precipitation Effects. *Energy Fuels* **2017**, *31* (12), 13144−13158.
(35) Rüger, C. P.; Miersch, T.; Schwemer, T.; Sklorz, M.; Zimmermann, R. Hyphenation of Thermal Analysis to Ultrahigh-Resolution Mass Spectrometry (Fourier Transform Ion Cyclotron Resonance Mass Spectrometry) Using Atmospheric Pressure Chemical Ionization For Studying Composition and Thermal Degradation of Complex Materials. *Anal. Chem.* **2015**, *87* (13), 6493−6499.
(36) Rüger, C. P.; Grimmer, C.; Sklorz, M.; Neumann, A.; Streibel, T.; Zimmermann, R. Combination of Different Thermal Analysis Methods Coupled to Mass Spectrometry for the Analysis of Asphaltenes and Their Parent Crude Oils: Comprehensive Characterization of the Molecular Pyrolysis Pattern. *Energy Fuels* **2018**, *32* (3), 2699−2711.
(37) Rüger, C. P.; Tiemann, O.; Neumann, A.; Streibel, T.; Zimmermann, R. Review on Evolved Gas Analysis Mass Spectrometry

with Soft Photoionization for the Chemical Description of Petroleum, Petroleum-Derived Materials, and Alternative Feedstocks. *Energy Fuels* **2021**, *35* (22), 18308−18332.
(38) Lack, D. A.; Moosmüller, H.; McMeeking, G. R.; Chakrabarty, R. K.; Baumgardner, D. Characterizing elemental, equivalent black, and refractory black carbon aerosol particles: a review of techniques, their limitations and uncertainties. *Anal. Bioanal. Chem.* **2014**, *406* (1), 99−122.
(39) Chow, J. C.; Watson, J. G.; Pritchett, L. C.; Pierson, W. R.; Frazier, C. A.; Purcell, R. G. The dri thermal/optical reflectance carbon analysis system: description, evaluation and applications in U.S. Air quality studies. *Atmospheric Environment. Part A. General Topics* **1993**, *27* (8), 1185−1201.
(40) Chow, J. C.; Watson, J. G.; Chen, L. W. A.; Chang, M. C. O.; Robinson, N. F.; Trimble, D.; Kohl, S. The IMPROVE_A temperature protocol for thermal/optical carbon analysis: maintaining consistency with a long-term database. *Journal of the Air & Waste Management Association (1995)* **2007**, *57* (9), 1014−1023.
(41) Chow, J. C.; Watson, J. G.; Crow, D.; Lowenthal, D. H.; Merrifield, T. Comparison of IMPROVE and NIOSH Carbon Measurements. *Aerosol Sci. Technol.* **2001**, *34* (1), 23−34.
(42) Diab, J.; Streibel, T.; Cavalli, F.; Lee, S. C.; Saathoff, H.; Mamakos, A.; Chow, J. C.; Chen, L.-W. A.; Watson, J. G.; Sippula, O.; Zimmermann, R. Hyphenation of a EC/OC thermal-optical carbon analyzer to photo-ionization time-of-flight mass spectrometry: an off-line aerosol mass spectrometric approach for characterization of primary and secondary particulate matter. *Atmos. Meas. Technol.* **2015**, *8* (8), 3337−3353.
(43) Grabowsky, J.; Streibel, T.; Sklorz, M.; Chow, J. C.; Watson, J. G.; Mamakos, A.; Zimmermann, R. Hyphenation of a carbon analyzer to photo-ionization mass spectrometry to unravel the organic composition of particulate matter on a molecular level. *Anal. Bioanal. Chem.* **2011**, *401* (10), 3153−3164.
(44) Streibel, T.; Schnelle-Kreis, J.; Czech, H.; Harndorf, H.; Jakobi, G.; Jokiniemi, J.; Karg, E.; Lintelmann, J.; Matuschek, G.; Michalke, B.; Müller, L.; Orasche, J.; Passig, J.; Radischat, C.; Rabe, R.; Reda, A.; Rüger, C.; Schwemer, T.; Sippula, O.; Stengel, B.; Sklorz, M.; Torvela, T.; Weggler, B.; Zimmermann, R. Aerosol emissions of a ship diesel engine operated with diesel fuel or heavy fuel oil. *Environ. Sci. Pollut. Res.* **2017**, *24* (12), 10976−10991.
(45) Miersch, T.; Czech, H.; Stengel, B.; Abbaszade, G.; Orasche, J.; Sklorz, M.; Streibel, T.; Zimmermann, R. Composition of carbonaceous fine particulate emissions of a flexible fuel DISI engine under high velocity and municipal conditions. *Fuel* **2019**, *236*, 1465−1473.
(46) Sippula, O.; Stengel, B.; Sklorz, M.; Streibel, T.; Rabe, R.; Orasche, J.; Lintelmann, J.; Michalke, B.; Abbaszade, G.; Radischat, C.; Gröger, T.; Schnelle-Kreis, J.; Harndorf, H.; Zimmermann, R. Particle emissions from a marine engine: chemical composition and aromatic emission profiles under various operating conditions. *Environ. Sci. Technol.* **2014**, *48* (19), 11721−11729.
(47) Kösling, P.; Rüger, C. P.; Schade, J.; Fort, K. L.; Ehlert, S.; Irsig, R.; Kozhinov, A. N.; Nagornov, K. O.; Makarov, A.; Rigler, M.; Tsybin, Y. O.; Walte, A.; Zimmermann, R. Vacuum Laser Photoionization inside the C-trap of an Orbitrap Mass Spectrometer: Resonance-Enhanced Multiphoton Ionization High-Resolution Mass Spectrometry. *Analytical chemistry* **2021**, *93* (27), 9418−9427.
(48) Giusti, P.; Bouyssière, B.; Carrier, H.; Afonso, C. 18th International Conference on Petroleum Phase Behavior and Fouling. *Energy Fuels* **2018**, *32* (3), 2641.
(49) Abivin, P.; Taylor, S. D.; Freed, D. Thermal Behavior and Viscoelasticity of Heavy Oils. *Energy Fuels* **2012**, *26* (6), 3448−3461.
(50) Kharrat, A. M.; Indo, K.; Mostowfi, F. Asphaltene Content Measurement Using an Optical Spectroscopy Technique. *Energy Fuels* **2013**, *27* (5), 2452−2457.
(51) Giraldo-Dávila, D.; Chacón-Patiño, M. L.; McKenna, A. M.; Blanco-Tirado, C.; Combariza, M. Y. Correlations between Molecular Composition and Adsorption, Aggregation, and Emulsifying Behaviors of PetroPhase 2017 Asphaltenes and Their Thin-Layer Chromatography Fractions. *Energy Fuels* **2018**, *32* (3), 2769−2780.
(52) Chow, J. C.; Wang, X.; Sumlin, B. J.; Gronstal, S. B.; Chen, L.-W. A.; Trimble, D. L.; Watson, J. G.; Kohl, S. D.; Mayorga, S. R.; Riggio, G.; Hurbain, P. R.; Johnson, M.; Zimmermann, R. Optical Calibration and Equivalence of a Multiwavelength Thermal/Optical Carbon Analyzer. *Aerosol Air Qual. Res.* **2015**, *15* (4), 1145−1159.
(53) Siskin, M.; Kelemen, S. R.; Eppig, C. P.; Brown, L. D.; Afeworki, M. Asphaltene Molecular Structure and Chemical Influences on the Morphology of Coke Produced in Delayed Coking. *Energy Fuels* **2006**, *20* (3), 1227−1234.
(54) Gray, M. R. Consistency of Asphaltene Chemical Structures with Pyrolysis and Coking Behavior. *Energy Fuels* **2003**, *17* (6), 1566−1569.
(55) Wu, X.; Vu, T. V.; Shi, Z.; Harrison, R. M.; Liu, D.; Cen, K. Characterization and source apportionment of carbonaceous PM2.5 particles in China - A review. *Atmos. Environ.* **2018**, *189*, 187−212.
(56) Watson, J. G.; Chen, L. W. A.; Chow, J. C.; Doraiswamy, P.; Lowenthal, D. H. Source apportionment: findings from the U.S. Supersites Program. *J. Air Waste Manage. Assoc.* **2008**, *58* (2), 265−288.
(57) Speight, J. G.; Long, R. B.; Trowbridge, T. D. Factors influencing the separation of asphaltenes from heavy petroleum feedstocks. *Fuel* **1984**, *63* (5), 616−620.
(58) Speight, J. G.; Long, R. B. THE CONCEPT OF ASPHALTENES REVISITED. *Fuel Science and Technology International* **1996**, *14* (1−2), 1−12.
(59) Gray, M. R.; Yarranton, H. W.; Chacón-Patiño, M. L.; Rodgers, R. P.; Bouyssiere, B.; Giusti, P. Distributed Properties of Asphaltene Nanoaggregates in Crude Oils: A Review. *Energy Fuels* **2021**, *35* (22), 18078−18103.
(60) Ibrahim, H. A.-H. Thermal Treatment of Syrian Sponge Coke. *Journal of King Saud University - Engineering Sciences* **2006**, *18* (2), 261−269.
(61) Siskin, M.; Kelemen, S. R.; Gorbaty, M. L.; Ferrughelli, D. T.; Brown, L. D.; Eppig, C. P.; Kennedy, R. J. Chemical Approach to Control Morphology of Coke Produced in Delayed Coking. *Energy Fuels* **2006**, *20* (5), 2117−2124.
(62) Dorset, D. L.; Siskin, M.; Brown, L. D. Molecular Assemblies in Asphaltenes and Their High-Temperature Coke Products. 2. Levels of Molecular Organization. *Energy Fuels* **2011**, *25* (10), 4580−4585.
(63) Alvarez, E.; Marroquín, G.; Trejo, F.; Centeno, G.; Ancheyta, J.; Díaz, J. A. Pyrolysis kinetics of atmospheric residue and its SARA fractions. *Fuel* **2011**, *90* (12), 3602−3607.
(64) Kök, M. V.; Karacan, O. Pyrolysis Analysis and Kinetics of Crude Oils. *J. Therm. Anal. Calorim.* **1998**, *52* (3), 781−788.
(65) Karacan, O.; Kök, M. V. Pyrolysis Analysis of Crude Oils and Their Fractions. *Energy Fuels* **1997**, *11* (2), 385−391.
(66) Alostad, L. K.; Palacio Lozano, D. C.; Gannon, B.; Downham, R. P.; Jones, H. E.; Barrow, M. P. Investigating the Influence of n -Heptane versus n -Nonane upon the Extraction of Asphaltenes. *Energy Fuels*, in press, **2022**.
(67) Cho, Y.; Kim, Y. H.; Kim, S. Planar limit-assisted structural interpretation of saturates/aromatics/resins/asphaltenes fractionated crude oil compounds observed by Fourier transform ion cyclotron resonance mass spectrometry. *Analytical chemistry* **2011**, *83* (15), 6068−6073.

https://doi.org/10.1021/acs.energyfuels.2c02122
Energy Fuels 2022, 36, 10177−10190